Similarity Solutions for Capillary Pinch-Off in Fluids of Differing Viscosity

Wendy W. Zhang[1] and John R. Lister[2]
[1]*Division of Engineering and Applied Sciences, Harvard University, Cambridge, Massachusetts 02138*
[2]*Institute of Theoretical Geophysics, DAMTP, Silver Street, Cambridge, CB3 9EW, United Kingdom*
(Received 25 March 1999)

Self-similar profiles associated with capillary instability of a fluid thread of viscosity $\lambda\eta$ in surrounding fluid of viscosity η are obtained for $\frac{1}{16} \leq \lambda \leq 16$ via a simplified numerical scheme. Universal similarity scaling is preserved despite an asymptotically large velocity in the pinching neck driven by nonlocal dynamics. The numerical results agree well with experimental measurements by Cohen *et al.* [preceding Letter, Phys. Rev. Lett. **83**, 1147 (1999)]. For all λ, the self-similar profile is asymmetric and conical far from the minimum. The steep cone slope increases monotonically with λ; the shallow cone slope is maximized around $\lambda = \frac{1}{4}$.

PACS numbers: 47.20.Dr, 47.11.+j, 68.10.–m

Resurgent interest in the classic fluid-mechanical problem of capillary pinch-off of a fluid thread, as recently reviewed in [1], has focused on analysis of the final stage of pinch-off. Theoretical motivation arises from general interest in the self-organization of nonlinear dynamics near finite-time singularities, such as topological transitions, and, in particular, with issues such as universality, scaling, and uniqueness [2,3]. Further motivation arises from diverse technological applications such as emulsification and spray production. Provided molecular dimensions are not reached first, viscous dissipation in the surrounding fluid, however small initially, is asymptotically dominant over inertia. Consequently, pinch-off in surrounding fluid of any viscosity eventually enters a self-similar regime in which the destabilizing capillary pressure is opposed by internal and external viscous dissipation [4–6]. In contrast to the usual assumption that the thread profile and flow field close to pinch-off are determined solely by local dynamics, viscous pinch-off of a thread in surrounding fluid involves an asymptotically large nonlocal contribution to the flow field in the pinching neck. Here we show how to account for this nonlocal contribution and examine the effect of the viscosity ratio on the self-similar pinching structure.

Consider a fluid thread of viscosity $\lambda\eta$ and surface tension γ, pinching in surrounding fluid of viscosity η. Under capillary pressure, nonaxisymmetric deformations can be expected to decay more rapidly than the thread pinches; thus only axisymmetric profiles need to be considered. Let the thread have radius $h(z,t)$, where z is the axial coordinate, and t is the time to pinch-off. To see how h and z scale with t, note first that in Stokes flow the pressure and velocity fields are both determined by equidimensional Laplacian operators, and thus when only free-surface boundaries are present there is no preferred direction. This suggests that $h \sim z$ as $t \to 0$. Balancing internal and external viscous stresses against capillary pressure yields the estimate $u \sim \gamma/\eta$, which suggests that the velocity is constant as $t \to 0$. Hence, $h, z \sim t$; the Reynolds number $\mathrm{Re} = \rho u h/\eta \propto t$, where ρ is the density, which is consistent with the neglect of inertia. In accordance with the scaling arguments, we nondimensionalize all velocities by γ/η, lengths by an initial thread radius h_0, and time to rupture by $\eta h_0/\gamma$. Henceforth, all variables are dimensionless.

The scaling arguments for h, z, and u were checked for $\lambda = 1$ pinch-off in Stokes-flow simulations which tracked the evolution of an initially deformed drop by using a boundary-integral method to solve for the interfacial velocity at each time step [5]. The simulations showed that h and z indeed decrease linearly with t and that the self-similar profile is conical away from $h_{\min}$. However, in disagreement with the simple scaling arguments, the axial velocity does not remain constant as $t \to 0$ but increases slowly like $|\ln t|$. Yet the axial strain $\partial_z u_z \sim 1/z \sim t^{-1}$ as expected.

Lister and Stone [5] demonstrated that the retraction of the far-field conical regions under capillary stresses creates a tug-of-war between the two cones, with the winning cone pulling the entire pinching neck toward itself, stretching out the cone on the opposite end. Thus the dynamics associated with Stokes-flow pinch-off has a nonlocal velocity component which, instead of being negligible as is usual close to a finite-time singularity, is asymptotically dominant over the locally driven contribution as $t \to 0$. Fortunately, this asymptotically large nonlocal contribution to the velocity in the neck is primarily a uniform advection, which does not deform the interface and therefore does not affect the local dynamics. The axial strain is dominantly locally driven and does not depend on the cone slopes s_+ and s_-. Thus the pinching rate and the thread profile can remain self-similar despite the asymptotically large nonlocal contribution to the velocity.

We anticipate that the self-similar profiles for $\lambda \neq 1$ pinch-off exhibit analogous behavior; i.e., the far-field cones contribute only uniform advection and the local profiles are insensitive to all other aspects of the nonlocal structure. Thus it is possible to simulate evolution towards

the self-similar structure in the pinching region by simply prescribing the surface profile at intermediate to macroscopic length scales at each time step. To do so, it is expedient to work with a rescaled thread radius $H(\zeta)$ and axial distance ζ,

$$H(\zeta) = \frac{h(z,t)}{h_{\min}(t)} \qquad \zeta = \frac{z - z(h_{\min})}{h_{\min}(t)}, \tag{1}$$

in effect changing to a self-similar reference frame which fixes the minimum radius $H = 1$ at $\zeta = 0$. The dynamics are unaffected by the moving origin of ζ since inertia is negligible.

In our simplified numerical scheme, only the central pinching neck is time-evolved accurately. The thread profile outside the neck is approximated beyond a large distance by circular cones which are closed off at even larger distances by spherical caps. The cones and caps are prescribed such that the interfacial slope is continuous at the points of attachment between the pinching neck, the cones, and the caps. The cones were typically attached onto the neck at $R_c = \sqrt{H^2(\zeta_c) + \zeta_c^2} = 10^3$ from the origin, and the caps were attached onto the cones at $R_s = 10^4$, i.e., at fixed distances from $h_{\min}$ in similarity variables but decreasing distances in the lab frame. This numerical procedure is entirely equivalent to the assumption of a far-field shape and velocity field required for solution of similarity equations on a truncated domain using Newton's method. Provided the truncation is done sufficiently far into the far-field, the errors are small.

With a closed interface specified as above, a standard boundary-integral method [7] is used to calculate the interfacial velocities. To resolve both the large-scale far-field and the local structure of the pinching neck, grid points were redistributed along the interface so that the spacing between points remained inversely proportional to the distance from the origin throughout a simulation. The thread profile is updated by moving the grid points in the pinching neck with the normal component of the calculated interfacial velocity, and then attaching new cones and caps according to the new, smaller value of $h_{\min}$. The time step was chosen such that $h_{\min}(t)$ decreased by about 1.5% at each step.

The convergence of the scaled thread profile to a steady self-similar shape was taken to be complete when parameters, such as the cone slopes and the axial curvature at $h_{\min}$, varied by less than 1% per decade of further reduction in $h_{\min}(t)$. Self-similar profiles for different λ were obtained successively from the self-similar profile from the full Stokes flow simulation for $\lambda = 1$ [5]: this was used as the initial condition for simplified simulations at $\lambda = 2$ and $\frac{1}{2}$; the self-similar profiles at $\lambda = 2$ and $\frac{1}{2}$ were then used as initial conditions for $\lambda = 4$ and $\frac{1}{4}$, etc. At $\lambda < \frac{1}{16}$, errors associated with the degenerate eigenmode in the singular $\lambda = 0$ limit became significant. At $\lambda > 16$, the thread profile evolution became oscillatory. For $\frac{1}{16} \le \lambda \le 16$, repeat calculations with different initial profiles or over a greater range of reduction in $h_{\min}$ yielded essentially the same results. Repeat calculations for $\lambda = \frac{1}{16}, 16$ with double the density of points and an appropriately reduced time step, and with the same density of points and halved time step, gave differences in results of 0.5%–3%. Tests with $R_c = 10^4$ and $R_s = 10^5$ showed that the errors due to truncation were typically less than 1%. The calculated self-similar profiles are thus thought to have this sort of accuracy.

We now turn to a discussion of the results. Figure 1 presents self-similar profiles for $\lambda = \frac{1}{16}$, $\frac{1}{4}$, 1, 4, and 16 in the pinching neck. For all λ, the profile is asymmetric and quickly becomes conical away from $h_{\min}$. The profiles vary nonmonotonically with λ, as discussed below. Figures 2 and 3 present the steep cone slope s_+, shallow cone slope s_-, and axial curvature $\kappa_2(\zeta) = H''/\sqrt{1 + H'^2}$ as a function of λ. The calculated slopes s_+ and s_- are in good agreement with the experimental measurements by Cohen *et al.* [8], given experimental uncertainties, except for s_+ at $\lambda \ll 1$.

Both the calculated s_- and $\kappa_2(0)$ have a maximum around $\lambda = \frac{1}{4}$ and the calculated s_+, though always increasing with λ, appears to change its λ dependence around $\lambda = \frac{1}{4}$ as well. The shift to longer length scales seen in the behavior of s_- and $\kappa_2(0)$ at large and small λ parallels that observed in the linear stability of a viscous fluid cylinder in another viscous fluid [9], for which the most unstable wave number has a maximum at $\lambda = 0.28$. Estimation of internal and external fluid stresses suggests that long-wavelength motions are generally preferred by such free-surface Stokes flows at extreme viscosity ratios. The shift of the pinching dynamics to longer length scales at large and small λ can also be seen in profiles of $\kappa_2(\zeta)$ for $\lambda = \frac{1}{16}$, $\frac{1}{4}$, 1, 4, and 16 (Fig. 3B): for $\lambda \ll 1$, this shift is accomplished primarily by a broadening of the peak in κ_2; for $\lambda \gg 1$, it is accomplished by shifting away from $h_{\min}$ of the peak marking the transition to the start of the steep cone.

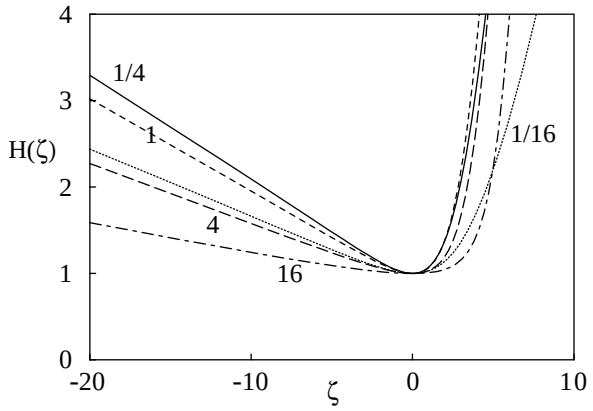

FIG. 1. Self-similar profiles for $\lambda = \frac{1}{16}$ (dotted line), $\frac{1}{4}$ (solid line), 1 (dashed line), 4 (long-dashed line), and 16 (dot-dashed line).

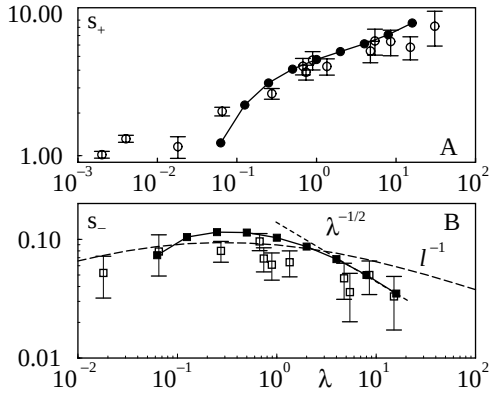

FIG. 2. Calculated steep cone slope s_+ (filled circles) and shallow cone slope s_- (filled squares) compared with the experimental measurements by Cohen *et al.* [8] (open circles and squares). The long-dashed curve corresponds to l^{-1}, where l is the linearly most unstable wavelength for a cylinder of viscous fluid immersed in another fluid [9].

The suggested $\lambda^{-1/2}$ scaling of s_- and λ^{-1} scaling of $\kappa_2(0)$ when $\lambda \gg 1$ can be rationalized by assuming long-wave dynamics and balancing the internal extensional stress $\lambda\partial_z(h^2\partial_z u_z)$ with external shear stresses $h\partial_r u_z$, as discussed in [5]. In hindsight, it is clear why attempts to capture pinch-off dynamics at large λ with a long-wave model was not successful, since the steep cone slope, somewhat surprisingly, becomes large at large λ. The observed trends at large λ indicate that the symmetric similarity solution for capillary pinching with zero exterior viscosity [10], obtained by assuming long-wave dynamics, does not constitute the proper limiting solution for $\lambda \to \infty$, probably due to the fact that the external viscous dissipation remains comparable to the internal dissipation even as $\lambda \to \infty$.

An examination of the flow fields presented in Figs. 4 and 5 yields some insights into the dynamics which give rise to the observed pinch-off profiles. To illustrate the deforming flow in the neck most clearly, in Fig. 4 we have adopted a reference frame translating axially with roughly half of the axial velocity of $h_{\min}$. (Recall that the large nonlocal component of the axial flow is uniform and nondeforming.) Figure 4 depicts flow fields for $\lambda = \frac{1}{8}$ and $\lambda = 8$. The $\lambda = 8$ velocity vectors have been nondimensionalized by $\lambda\eta$ instead of η since the larger viscosity presents the dominant resistance. The overall flow patterns are then similar: there is an almost spatially uniform radial flow towards the thread balanced by axial advection away from $h_{\min}$ close to and within the thread. As might be anticipated, there is a significant difference in the axial velocity profile in the shallow cone: the $\lambda = \frac{1}{8}$ profile is nearly parabolic in cross section; the $\lambda = 8$ profile is

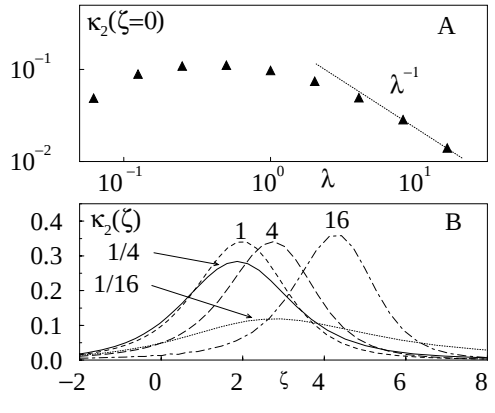

FIG. 3. Axial curvature $\kappa_2(\zeta) = H''/\sqrt{1 + H'^2}$. (A) $\kappa_2(0)$ as a function of λ; (B) profiles for $\lambda = \frac{1}{16}$ (dotted line), $\frac{1}{4}$ (solid line), 1 (dashed line), 4 (long-dashed line), and 16 (dot-dashed line).

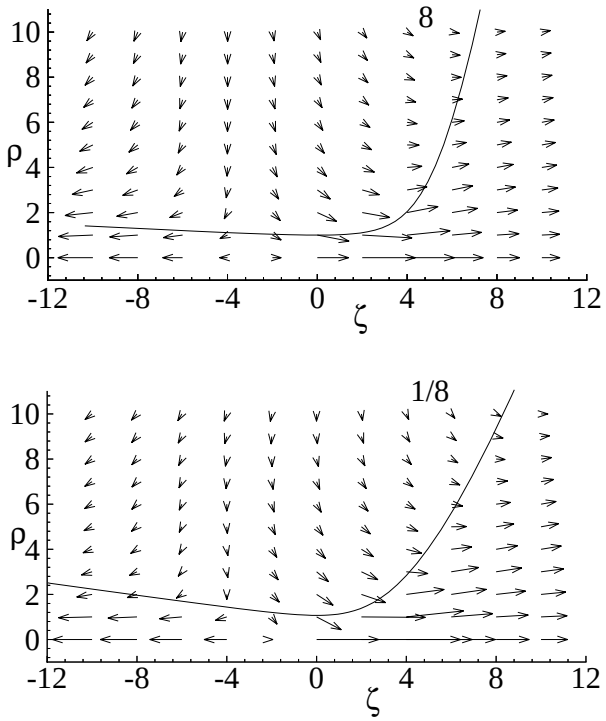

FIG. 4. Flow fields for $\lambda = 8$ (top) and $\lambda = \frac{1}{8}$ (bottom) in the reference frame with $u_z(4, 6) = 0$. Velocities for $\lambda = 8$ are nondimensionalized by $\lambda\eta$ instead of η. All velocity vectors are magnified by 4.

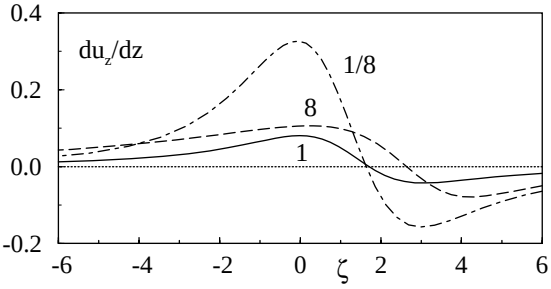

FIG. 5. The axial strain on the thread centerline for $\lambda = \frac{1}{8}$ (dot-dashed line), 1 (solid line), and 8 (dashed line). Strains for $\lambda = 8$ are nondimensionalized by $\lambda\eta$ instead of η.

nearly uniform. The flow in the retracting steep cone is more complicated.

In addition to the uniform axial velocity towards the steep cone driven nonlocally by the far-field conical profiles, the thread surface is rolling: the local flow pushes the steep cone downward and tilts the shallow cone upward, resulting in an axial shift of $h_{\min}$ towards the steep cone. The deforming flow also stretches out the shallow cone and compresses the steep cone, as can be seen most easily in a plot of the axial strain along the thread centerline (Fig. 5).

Figure 6 presents a comparison of the calculated self-similar pinching rates $dh_{\min}/dt$ with experimental measurements [8]. As noted by [8], the self-similar pinching rate is well approximated for $0.1 < \lambda < 4$ by the maximum growth rate from linear stability analysis of a viscous cylinder in another viscous fluid [9]. This is consistent with Fig. 2, in which, over the same range of λ, s_- matches l^{-1} almost exactly, where l is the linearly most unstable wavelength.

It is tempting to define $l_s = 1/s_-$ as the characteristic distance over which the shallow cone looks like a cylinder on the $O(h_{\min})$ scale and, ignoring the steep cone, then argue that when $l_s \sim l$ the pinching dynamics in the self-similar reference frame is analogous to the initial instability of a perturbed cylinder. However, this would not explain why the agreement fails at large and small viscosity ratios, when s_- is smaller and therefore looks even more cylindrical on the $O(h_{\min})$ length scale. Moreover, it would be equally sensible to define $l_\kappa = \kappa^{-1/2}$, where κ is either the maximum axial curvature or $\kappa_2(0)$. In both cases, $l_\kappa \ll l$ suggesting that the region about $h_{\min}$ does not look particularly like a cylinder. As $dh_{\min}/dt$ is more likely to be determined locally than slaved to the thinning of the shallow cone, l_κ appears to be a more relevant length scale than l_s, in which case the close agreement between linear stability results and self-similar pinching would be simply fortuitous. A more quantitative examination of the analogy between the pinching thread and linear stability of a cylinder would clearly be helpful.

In conclusion, the self-similar structure associated with capillary pinch-off of a fluid thread in surrounding fluid is embedded in an asymptotically large advection induced by structure on length scales much larger than the characteristic $O(h_{\min})$ local length scale and much smaller than the macroscopic drop size. However, as the nonlocal contribution to the velocity field in the pinching region is nearly uniform, the self-similarity of the pinching dynamics is preserved. Results for thread pinch-off at $\lambda = \frac{1}{16}$ to 16 are presented and shown to be consistent with experimental measurements [8]. At all λ, the self-similar profile is asymmetric and conical away from $h_{\min}$. For $\lambda \gg 1$, which corresponds to the pinching of a syrup thread in air, the self-similar profile has a steep cone on one side of $h_{\min}$ and a shallow cone on the other. For $\lambda \ll 1$, which corresponds to the pinching of an elongated air bubble in syrup, the self-similar profile has shallow cones on both sides of $h_{\min}$. The observed λ dependence, in particular the flattening of the shallow cone at large λ and the flattening of both cones at small λ, is partially explained by analogy with linear stability results, but the steepening of the steep cone at large λ is a surprise.

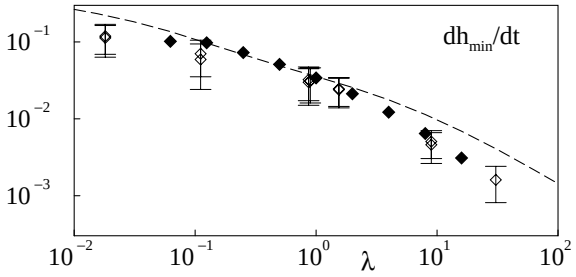

FIG. 6. Comparison of calculated $dh_{\min}/dt$ (filled diamonds) with experimental measurements (open diamonds). The dashed curve corresponds to the maximum growth rate predicted by linear stability analysis of a cylinder of viscous fluid in viscous surroundings [9].

The authors are grateful to I. Cohen, M. P. Brenner, J. Eggers, and S. R. Nagel for sharing their ideas and their experimental data with us. We are indebted to H. A. Stone for providing us with an initial version of the boundary-integral code. W. W. Zhang thanks T. R. Powers for helpful discussions and acknowledges financial support from NSF and the Harvard MRSEC (grant to H. A. Stone).

[1] J. Eggers, Rev. Mod. Phys. **69**, 865 (1997).
[2] See, e.g., *Singularities in Fluids, Plasmas, and Optics*, edited by R. E. Caflisch and G. C. Papanicolaou (Kluwer, Norwell, MA, 1993).
[3] A. L. Bertozzi, M. P. Brenner, T. F. Dupont, and L. P. Kadanoff, in *Trends and Perspectives in Applied Mathematics*, edited by L. Sirovich (Springer, New York, 1994).
[4] J. R. Lister, M. P. Brenner, R. F. Day, E. J. Hinch, and H. A. Stone, in *Proceedings of the IUTAM Symposium on Non-linear Singularities in Deformation and Flow, Haifa, Israel, 1997*, edited by D. Durban and J. R. A. Pearson (Kluwer, Norwell, MA, 1999).
[5] J. R. Lister and H. A. Stone, Phys. Fluids **10**, 2758 (1998).
[6] J. Blawzdziewicz, V. Cristini, and M. Loewenberg, Bull. Am. Phys. Soc. **42**, 2125 (1997).
[7] H. A. Stone and L. G. Leal, J. Fluid Mech. **220**, 161 (1990).
[8] I. Cohen, M. P. Brenner, J. Eggers, and S. R. Nagel, preceding Letter, Phys. Rev. Lett. **83**, 1147 (1999).
[9] S. Tomotika, Proc. R. Soc. Lond. A **150**, 322 (1935).
[10] D. Papageorgiou, Phys. Fluids **7**, 1529 (1995).